FDTD analysis of nano-antenna structures with dispersive materials at optical frequencies

José M. Rico-García, José M. López-Alonso, Javier Alda

School of Optics, University Complutense of Madrid,
Av. Arcos del Jalón s/n, 28037 Madrid, Spain
Phone: +34 91 394 68 72, Fax: +34 91 394 68 85
E-mail: jmrico@fis.ucm.es jmlopez@opt.ucm.es, j.alda@fis.ucm.es

ABSTRACT

The Finite-Difference Time Domain method has encountered several difficulties when analyzing dispersive materials. This is the case of the metal structures that configure an optical antenna. These devices couple the electromagnetic radiation to conform currents that are rectified by another physical element attached to the antenna. Both elements: antenna and rectifier configures an optical detector with sub-wavelength dimensions. In this contribution we analyze the effect on the currents induced by the incident electromagnetic field using FDTD and taking into account the dispersive character of metal at optical frequencies. The analysis is done in a 2 dimensional framework and it serves as an analytical tool for the election of material and structures in the fabrication of optical antennas.

1. INTRODUCTION

An optical antenna is a detection device, both in the IR and in the visible, working in the same fashion as a radio-antenna does in the microwave range[1]. It is composed of two different elements: a planar, micron-sized, metallic structure deposited over a dielectric substrate - the antenna - and a rectifying element, commonly a microbolometer or a metal-oxide-metal (MOM) diode. They play two roles in the detection mechanism. The metallic structure couples the electromagnetic radiation to the rectifier, which provides a DC signal proportional to the energy of the oscillating currents induced by the incoming radiation (*see Fig. 1*). The performance of the detector in the IR is not the same as in the visible[2]. Nevertheless, the signal supplied by an antenna designed to work optimally in the IR when it is illuminated with visible light can be strong enough to be useful.

Because of the wavelength-sized nature of the device, a rigorous approach to solve Maxwell equations is required. Moreover, a realistic model of the metal should be taken into account. One of the most versatile methods employed to study such a problem is the Finite-Difference Time-Domain Method (FDTD). It consists in changing the derivatives in Maxwell equations by finite differences in a discrete grid[3]. Thus, the numerical scheme recovers the exact propagation and interaction of the electromagnetic fields with the scatterers and materials involved in the computation, except for the unavoidable effects of the discrete approximation to a set of continuous equations.

Nanotechnology II, edited by Paolo Lugli, Laszlo B. Kish, Javier Mateos,
Proceedings of SPIE Vol. 5838 (SPIE, Bellingham, WA, 2005)
0277-786X/05/$15 · doi: 10.1117/12.608708

On the other hand, metals at optical frequencies exhibit very different properties than dielectrics at the same frequencies. They are strongly dispersive and, specifically, the real part of their dielectric function is negative, which explains the high reflectivity they have in common in the visible part of the spectrum.

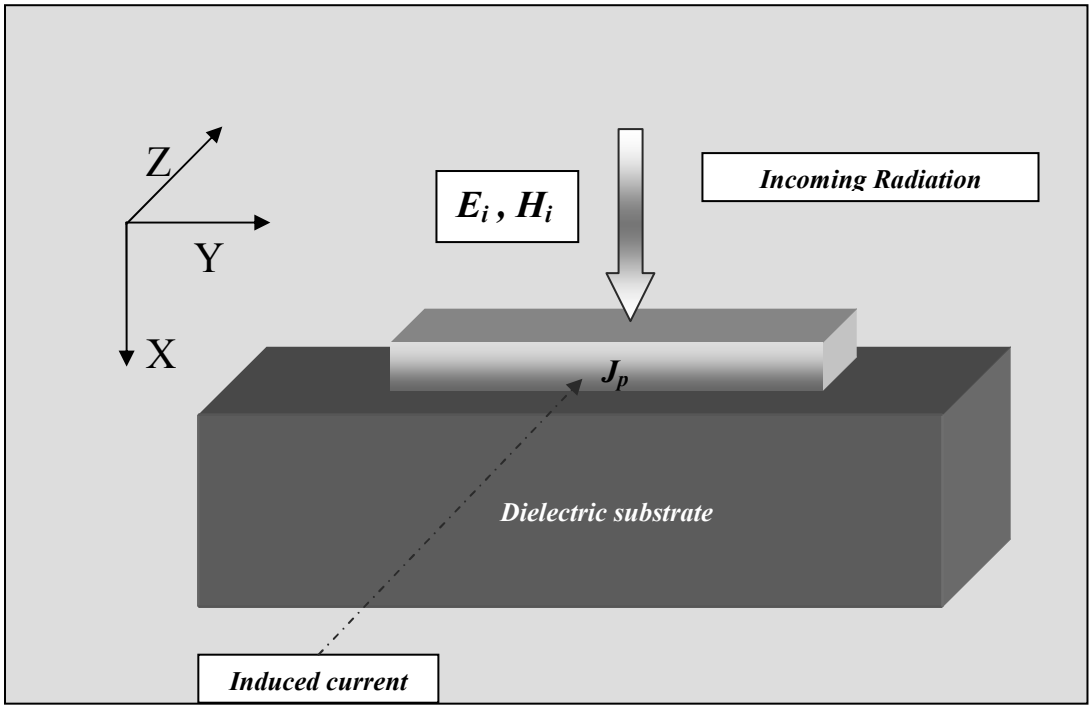

Figure 1. Scheme of excitation of the antenna-coupled detector. Light impinges over the thin metal layer, generating induced electric currents, $\boldsymbol{J_p}$*, through the layer volume. These currents are rectified by a diode or a microbolometer. The lateral dimensions of the antenna are comparable to the wavelength*[4]*. The thickness of the metal ribbon is typically 100 nm.*

To properly adapt FDTD schemes to these materials, the habitual equations must be altered. Furthermore, the accustomed formulations of FDTD fail if a phenomenological conductivity is introduced into the differences equations. The algorithm becomes unstable[5]. The right way to include into the FDTD computations the electric properties of metals at optical frequencies is to couple the Maxwell equations to a differential equation for the evolution of the material polarization[6].

2. FDTD APPROACH

We follow reference 6 in this section. We solve Maxwell equations in a two-dimensional grid. In 2D, the Maxwell equations decouples in two different polarizations, TM and TE. Choosing the former, Maxwell equations read as:

$$\partial_t H_x = \frac{1}{\mu_0}(-\partial_y E_z) \ , \qquad (1.1)$$

$$\partial_t H_y = \frac{1}{\mu_0}(\partial_x E_z) \ , \qquad (1.2)$$

$$\partial_t E_z = \frac{1}{\varepsilon_\infty}(\partial_x H_y - \partial_y H_x) - \frac{1}{\varepsilon_\infty} J_p \ . \qquad (1.3)$$

We adopt a simplified model of the antenna as a 2D structure because we are interested in the effect of the realistic model of the metal in the induced currents on the antenna structure. In spite of this, it would be computationally cheaper to have an estimation of the enhancement in the magnitude of these currents when a Fresnel lens is used to concentrate energy in the antenna plane[7].

To provide the correct index of refraction of the metal at the working frequency, avoiding any computational problem, we should include an extra equation to describe the effect of the material polarization in the scattered fields. The strategy is to fit the dielectric function of the metal at that frequency to a Debye or a Lorentz model of the index. This is done as follows,

$$\partial_t^2 P_z + \Gamma \partial_t P_z = (\varepsilon_0 \chi_0 E_z - P_z)\omega_0^2 \qquad , \qquad (2)$$

The parameters from the fitting are related to the constant coefficients of this differential equation based in a Lorentz model. P_z is the polarization of the metal; ε_0 is the vacuum permittivity; ω_0 is the resonance frequency; Γ is the damping coefficient, related to the quality factor of the resonance, and χ_0 is the polarizability at DC. These quantities are fixed after the fitting to the measured index of refraction. It is noticeable that there are four parameters to be fixed, and only two values from measurements (the refractive and the absorptive part of the index). This implies that two of them must be reasonably chosen by the user. The model can be easily integrated into the FDTD if we define the polarization current, $\boldsymbol{J_p}$, which represents the current induced in the metal by the incident field as:

$$J_p = \partial_t P \qquad . \qquad (3)$$

The permittivity, ε_∞, appearing in the equations (1.1), (1.2), and (1.3) is the limit when $\omega \rightarrow \infty$ in the Lorentz model, and its value is also derived from the fitting procedure[6]

Equations (1.1), (1.2), (1.3), (2) and (3) are integrated in a staggered grid, following a leap-frog scheme[3] consistently. A quasimonochromatic plane wave is allowed to excite the metallic ribbon. It is launched into the grid making use of a Total field / Scattered field zoning of the computational domain[3]. A customized uniaxial perfect matched layer[3] absorbs the outgoing waves scattered by the structure (*see Fig.2*). The fields are recorded both in the total field zone and the scattered field area. The spatial step is 6×10^{-9}, and the Courant factor is 0.6. The size of the computational grid is 529×1790 cells.

3. RESULTS

The geometry studied is schematized in Figure 1. The dimensions of the metal layer are 108 nm thick and 10 μm long. The dielectric substrate is assumed semi-infinite. We have calculated the fields both in the visible and in the infrared to estimate the coupling to the structure of the electromagnetic radiation when different wavelengths illuminate the device.

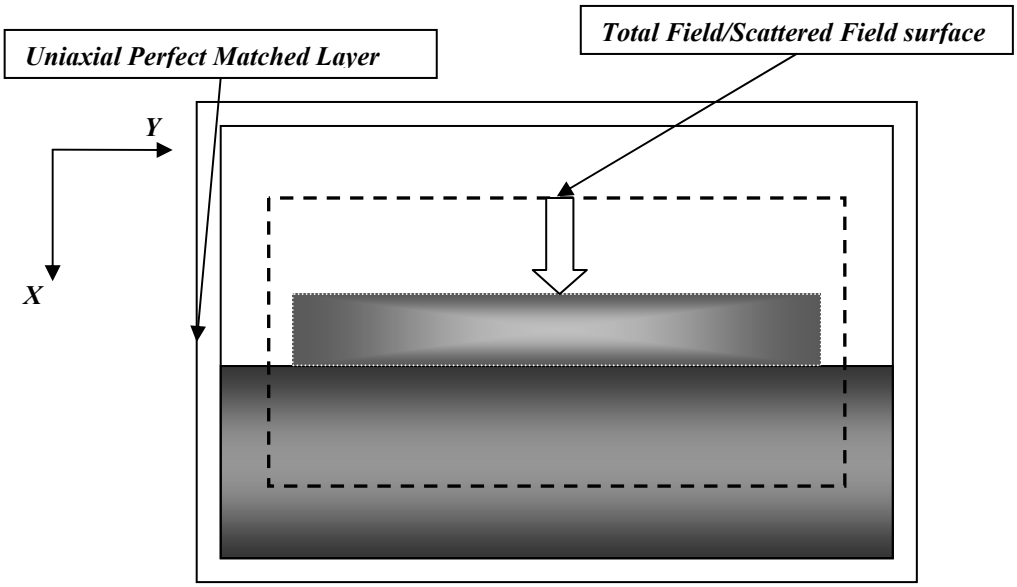

Figure 2: FDTD 2D model of the studied structure. An absorbing boundary condition surrounds the computational domain. A quasimonochromatic plane wave is injected in the grid through a Total Field/ Scattered Field surface. It travels perpendiculary to the y axis

Wavelength	$n_{measured}$	Γ *(Hz)*	ω_0 *(Hz)*	ε_∞	χ_0
780 nm	*0.175-4.91j*	4.153×10^{13}	2.066×10^{15}	*2.89*	*10*
10.628 μm	*12.65-65.41j*	1.02×10^{13}	1.6405×10^{14}	*1.8*	*800*

Table 1: Fitting parameters from the Lorentz model (See ref. 6)

We have fitted the index of refraction of gold at 10.6 μm and 780 nm[8,9]. The data from the fitting are shown in Table 1.

The spatial step has been chosen enough small to describe accurately the field propagation and interaction with the antenna.

Figure 3 shows a snapshot of the electric field when a plane wave oscillating at visible frequencies illuminates the antenna. It should be noted the penetration of the field in the thin metal. This effect can't be taken into account if it is not included the realistic model of the metal. The split of the grid into a total field zone and a scattered field zone is noticeable. A large amount of energy is reflected backwards, as expected from the high reflectance of noble metals at optical frequencies. The scattered field is, basically, the reflected wave by the metal except for slightly deformations created by the corners of the metallic structure.

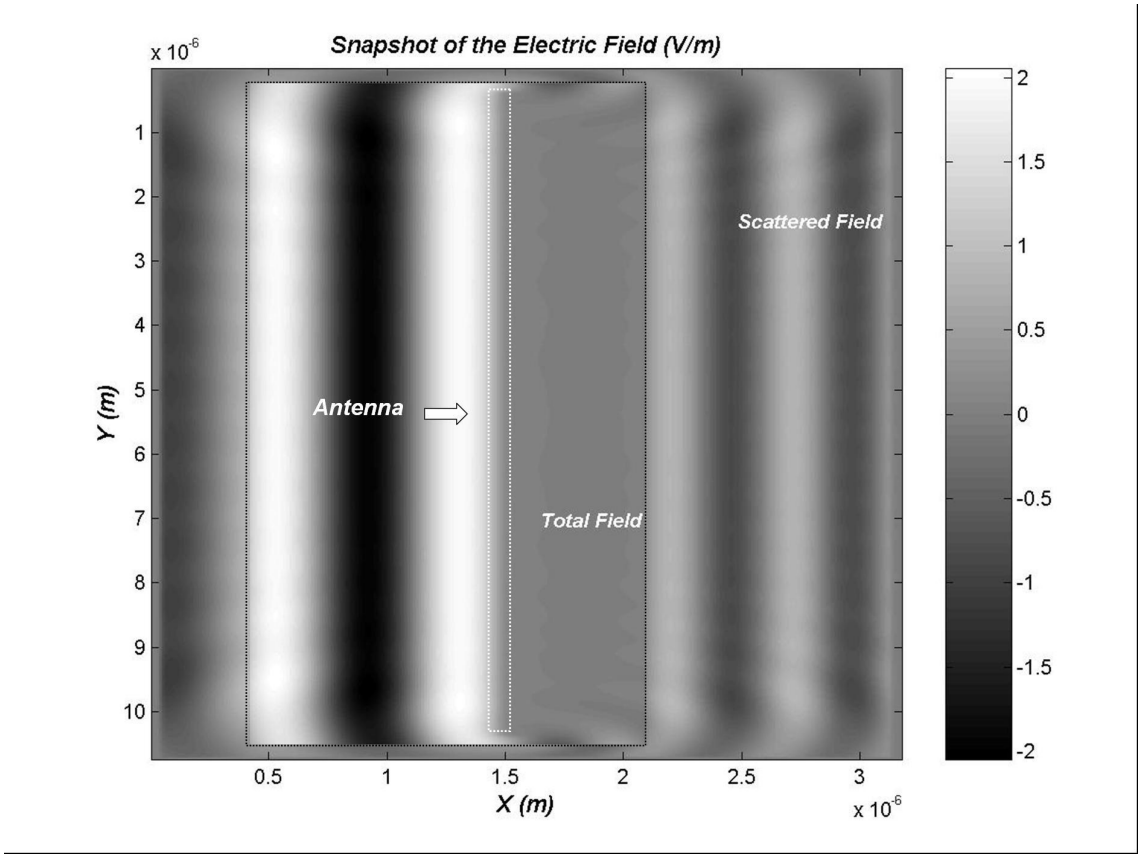

Figure 3: Snapshot of the electric field. The plane wave impinges normally to the antenna plane. λ = 780 nm. The maximum amplitude of the field is 1. As it can be seen, a large amount of the radiation is reflected backwards. The presence of the electric field in the back- scattered zone is not an error. The $\boldsymbol{E}_{scattered}$ *musts be ~ -* $\boldsymbol{E}_{incident}$ *to make zero the total field behind the antenna. The index of refraction of the dielectric is 1.511. The units of the electric field are V/m*

To compare the performance of the antenna working at different frequencies, we have recorded both in the visible and the IR the induced currents inside the antenna. As it has been explained above, the rectification of these currents gives raise to a DC signal, which is the final stage of the detection process at the device level. Thus, the larger the induced currents, the better the quality of the DC signal.

Figure 4 shows the temporal evolution of the current in the center of the antenna for the infrared excitation. To characterize and compare both cases, a Fast Fourier Transform is applied to the current for the IR and the visible. We pick up the Fourier component at the frequency of excitation for both cases and compute the quotient as a measure of the relative importance of one against the other

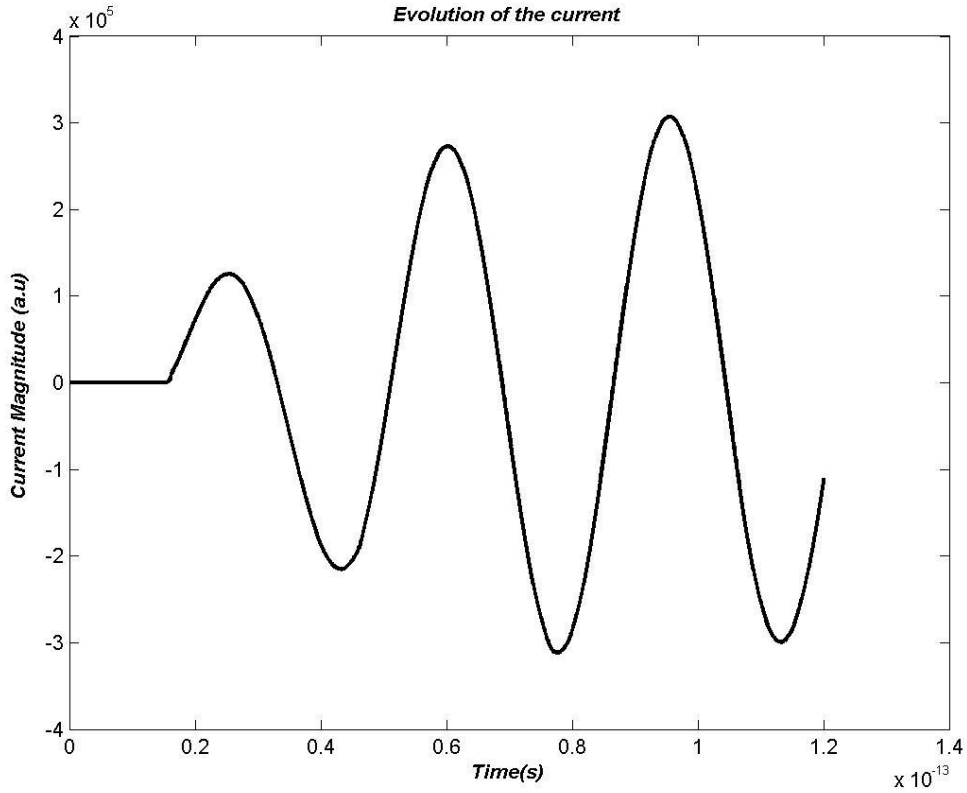

Figure 4: Time evolution of the induced current at the center of the antenna. (λ_{exc} = 10.628 μm, and the index of refraction of the dielectric substrate is 3.42, which is the index of Si at this wavelength)

$$\frac{Jp_{\max}(IR)}{Jp_{\max}(Visible)} = 30.5525 \qquad \textbf{(4)}$$

which means that the antenna performs better at IR frequencies than in the visible.

4. CONCLUSIONS

A simple 2D model for an optical antenna has been developed. It recovers the basic features of the interaction of radiation at infrared and visible frequencies with subwavelength structures. It takes into account, in a realistic manner, the dielectric properties of metals at optical frequencies, avoiding at the same time the instabilities generated by incorrect formulations of the FDTD algorithm. The properties of the metal have been included adding an extra equation to the previous set. The key is to adopt a Lorentz model for the index of refraction of the metal. A fitting of its parameter to the real and absorptive part of the index determines the constant coefficients of the differential equation for the polarization of the model. Then, the induced current, which is rectified by a suitable element (nanometer diode or microbolometer), is easily computed as the derivative of the polarization.

Two different computations have been carried out. They prove that the simplified model of the antenna works better at infrared frequencies than at visible frequencies. The peak current value at visible frequencies is minor than its counterpart at IR frequencies, suggesting a modification in the design of the antennas to improve their characteristics at those wavelengths.

ACKNOWLEDGMENTS

This work has been partially supported by project TIC2001-1259 from the Ministerio de Ciencia y Tecnología of Spain, and by the project GR/MAT/0497/2004 of the Comunidad de Madrid, Spain.

REFERENCES

1.- G.Boreman "Divide and conquer" *OE Mag.* **2** 47–8, (2002)

2.- C.Fumeaux, J.Alda, G.Boreman, "Lithographic antennas at visible frequencies", *Opt.Lett.* **24**, 1629-31 (1999).

3.- A. Taflove and S. C. Hagness *Computacional Electrodynamics: The Finite-Difference Time Domain Method*, 2nd ed. (Artech House, Boston, 2000).

4.- I.Codreanu, G.Boreman, “Infrared microstrip dipole antennas- FDTD prediction versus experiment”, *Microwave Opt. Technol. Lett.*, ***29***, 381-383, (2001).

5.- K.S.Kunz, R.J.Luebbers, *The Finite Difference Time Domain Method for Electromagnetics*, Boca Ratón, Fl, CRC, 1993.

6.- J.B.Judkins, R.W.Ziolklowski, “ Finite-Difference Time-Domain Modeling of Nonperfectly Conducting Metallic Thin-Film Gratings”, J. Opt. Soc. Am. A, **12,** 1974-1983, (1995).

7.- F.J.González, J.Alda, B. Ilic, G.Boreman, “Infrared antennas coupled to lithographic Fresnel Zone Plates ”, *App. Opt.* **43**, 6067-73. (2004)

8.- P.B.Johnson, R.W.Christy, “Optical constants of noble metals”, *Phys .Rev .B*, **6,** 4370-4379 (1972)

9.- Heather Verdeck, G. Boreman, “Constants of 100 nm thin layer of Gold in the infrared” Private communication (2005)